Composition, structure and properties of POPC–triolein mixtures. Evidence of triglyceride domains in phospholipid bilayers

CrossMark

Lars Duelund [a],*, Grethe Vestergaard Jensen [b],[1], Hans Kristian Hannibal-Bach [c], Christer S. Ejsing [c], Jan Skov Pedersen [b], Kirsi Inkeri Pakkanen [d], John Hjort Ipsen [a]

[a] MEMPHYS — Center for Biomembrane Physics, Department of Physics, Chemistry and Pharmacy, University of Southern Denmark, Odense M, Denmark
[b] Department of Chemistry and Interdisciplinary Nanoscience Center (iNANO), Aarhus University, Aarhus, Denmark
[c] Department of Biochemistry and Molecular Biology, University of Southern Denmark, Odense M, Denmark
[d] Department of Mechanical Engineering, Technical University of Denmark, Kgs. Lyngby, Denmark

ARTICLE INFO

ABSTRACT

We have in this study investigated the composition, structure and spectroscopical properties of multilamellar vesicles composed of a phospholipid, 1-palmitoyl-2-oleoyl-sn-glycero-3-phosphocholine (POPC), and up to 10 mol% of triolein (TO), a triglyceride. We found in agreement with previous results that the mixtures with 10 mol% TO spontaneously separate into two distinct phases, heavy (HF) and light (LF), with different densities and found this also to be the case for 2 and 5 mol% TO. The compositions of the two phases were investigated by quantitative lipid mass spectrometric analysis, and with this method we found that TO had a solubility maximum of about 4 mol% in the HF, whereas it was markedly up-concentrated in the LF. Electron paramagnetic resonance spectroscopy indicated POPC membranes of all tested concentrations of TO in both phases to be almost unperturbed by the presence of TO and to exist as vesicular structures containing entrapped water. Bilayer structure of the membranes was supported by small angle X-ray scattering that showed the membranes to form a lamellar phase. Fluorescence spectroscopy with the polarity sensitive dye Nile red revealed, that the LF samples with more than 5 mol% TO contained pure TO domains. These observations are consistent with an earlier MD simulation study by us and our co-workers suggesting triglycerides to be located in lens shaped, blister-like domains between the two lipid bilayer leaflets (Khandelia et al. (2010) [26]).

© 2013 Elsevier B.V. All rights reserved.

1. Introduction

Triglycerides, or triacylglycerides (TG), are well known neutral lipids that are the main components of fats and oils. They are formed by esterification of three fatty acids to a glycerol molecule, resulting in an extremely apolar molecule. In nature, TGs are important as nutritional compounds functioning as energy storage molecules for cells and organisms. In cellular conditions TGs are typically found encapsulated in lipid droplets, where a fluid TG core is covered by a phospholipid monolayer decorated with a number of specialised proteins [1–3]. Similar architecture for protecting highly apolar TGs is found in the blood: TGs circulating in the blood stream are built into lipoprotein particles with a TG core and covered by a proteolipid monolayer [4,5]. Partly due to their role as energy storage molecules and partly based on their sheltered location in biological environments, TGs are generally not considered to be a part of biological lipid membranes.

Some considerations on the biological role of TGs in lipid membranes have though been presented. The endoplasmic reticulum membrane where lipid droplets are formed is known to contain TGs [6,7]. Lysosomal membranes [8,9], as well as the lamellar bodies of lung surfactants [10] have also been shown to contain TGs. Nevertheless, the classical view of biological lipid membranes as being mainly composed of phospholipids and cholesterol has not considered the presence or effect of TGs on the properties or the organisation of the membranes.

The earliest suggestions for a possible role of TGs in the architecture of biological membranes were made in the 1980s by Mountford and co-workers who suggested the existence of TG domains in the plasma membranes of malignant cancer cells [11]. This suggestion was based on the observation of anisotropic, fast moving, and therefore narrow ^{1}H-NMR signals originating from TGs in membranes [11,12]. The location of the TG in the membranes was suggested on the basis of the influence of the membrane impermeable Gd^{3+} on the NMR signal [12]. The matter was debated in the literature, and evidence both in favour [13] and against [14] the membrane location of the TGs was given. It is likely that the mobile NMR signal arises both from TGs in the plasma membrane and in lipid droplets [15], but the subcellular origin of the NMR signal is still discussed [16].

 * Corresponding author. Tel.: +45 65502588.
   URL: lad@memphys.sdu.dk, http://www.memphys.dk (L. Duelund).
 [1] Current address: Niels Bohr Institute, University of Copenhagen, Frederiksberg C, Denmark.

Studying model mixtures has been a successful approach for understanding the physical chemistry and the interactions of the lipids in the cell membrane and has aided immensely in understanding the role of critical components like cholesterol in membranes (see e.g. [17,18]). However, for TG only a few studies have been undertaken. In the 1980s Hamilton and co-workers made a series of investigations on the interaction between TG and phospholipids by ^{13}C-NMR [19–21]. They found that the triolein (TO) has a limited solubility of 2–4 mol% in the membrane, which was further lowered in the presence of cholesterol esters [22]. Similar results have been obtained later for TG with mixed acyl chains [23] and for mixtures of 1-palmitoyl-2-oleoyl-sn-glycero-3-phosphocholine (POPC) and triolein (TO) by the studies of POPC monolayers at the air–water interface [24].

Recently, we have investigated POPC membranes containing 10 mol% triolein (TO) by various biophysical methods [25–27]. We initially observed that upon centrifugation or overnight storage this mixture separated into two phases that were named light (LF) and heavy (HF) phase in accordance with their sedimentation behaviour. The two phases showed very different behaviours when investigated with electron paramagnetic resonance spectroscopy (EPR) and fluorescence spectroscopy in the form of Laurdan GP. In contrast to this, almost no influence of TO on the phase transition of the POPC was found, and by the use of thin-layer chromatography (TLC) no significant difference in composition could be detected [25]. In subsequent work we showed that the presence of TO in the POPC membrane significantly lowered the bending rigidity and strongly affected the large scale morphology of electroformed or spontaneously swollen giant unilamellar vesicles (GUVs). In the same work we showed that the presence of TO did slightly increase the lamellar spacing, but did not make the vesicles more prone to fusion [27]. In order to gain further insight into the molecular organisation of the POPC–TO mixtures, molecular dynamics simulations were used [26]. These simulations showed that at low concentrations of TO, 2.3 mol%, all the TO molecules were placed in the membrane with their glycerol backbones at the membrane–water interface and the fatty acid chains parallel to the fatty acids of the POPC. At a higher concentration of TO, 5.3 mol%, the main part of TOs was found in lens shaped blisters between the two POPC leaflets. The TOs in the blisters were in a fluid and almost isotropic phase, with a random orientation of the fatty acid chains. Further, it was found that the system was very dynamic, allowing the TOs to flip-flop between the leaflets of the membranes at a rate of around 1 flip-flop per μs.

In this paper, we return to elucidate and elaborate the macroscopical phase separation of TO–POPC membranes and to obtain experimental evidence for the formation the TG blisters in the membranes. Our aim is to show and explain the structure–composition–behaviour relationship underlying the formation of the light and heavy phases of TO–POPC membranes. We want to present, with the help of more sophisticated methods, our improved understanding on, how and why the TO–POPC membranes are formed in two different variants with different physical properties. In addition to fundamental understanding of TOs' role as a membrane component our results will also give new insights into the formation and properties of lipid droplets and lipoprotein particles.

2. Materials and methods

2.1. Materials

1-Palmitoyl-2-oleoyl-sn-glycero-3-phosphocholine (POPC), 1-palmitoyl-2-stearoyl-(5-doxyl)-sn-glycero-3-phosphocholine (5-PC) and 1-palmitoyl-2-stearoyl-(16-doxyl)-sn-glycero-3-phosphocholine (16-PC) were from Avanti Polar Lipids (Alabaster, AL, USA). 1,2,3-Tri(cis-9-octadecenoyl)glycerol (triolein, TO), Triton X-100, methyl-5-doxylstearic acid spin-label (Me-5-DSA), methyl-16-doxylstearic

acid spin-label (Me-16-DSA), $K_3[Cr(Ox)_3]$ and all the salts were from Sigma Aldrich (St. Louis, MO, USA). CHCl$_3$ was from Rathburn Chemicals (Mikrolab, Aarhus, Denmark). Tempamine (TA, 4-amino-2,2,6,6-tetramethylpiperidinyloxy) was from Fluka (Sigma Aldrich, St. Louis, MO). The fluorescent probe Laurdan (6-dodecanoyl-2-dimethylaminonaphthalene) was from Invitrogen (Life Technologies Ltd., Paisley, UK) and Nile red (9-diethylamino-5-benzo[α] phenoxazinone) from Sigma Aldrich (St. Louis, MO, USA). All water used in this study was of ultra pure grade (18.2 MΩ cm) produced by a Millipore A10 Academic unit (Millipore Corp., Billerica, MA, USA).

2.2. Lipid suspensions

Unless otherwise noted, all lipid suspensions were prepared with a total lipid concentration of 10 mM by mixing the lipids and probes from chloroform stock solutions. Chloroform was removed by a gentle stream of nitrogen in a Stuart sample concentrator (VWR — Bie & Berntsen, Copenhagen, Denmark) and samples were then placed under reduced pressure overnight. Samples were hydrated with ultra pure water and multilamellar vesicles (MLVs) were formed by shaking the samples in an Eppendorf Thermomixer (Eppendorf AG, Hamburg, Germany) at 25 °C for 30 min. Unless otherwise noted, the heavy (HF) and light (LF) phase of the samples were separated by centrifugation for 30 min at 20,000 g in a Thermo Electron CR3i centrifuge (Holm & Halby, Brøndby, Denmark). The supernatant was aspired and used for the measurements as the LF phase. The pellet was suspended in water, in a volume corresponding to that of the removed supernatant. This resuspended pellet was used in the experiments as the HF phase.

2.3. Mass spectrometric lipid analysis

LF and HF were diluted in methanol and spiked with 150 pmol of internal standard TG 17:1/17:1/17:1 and PC 18:3/13:3. Samples were subsequently analysed in positive ion mode by direct infusion mass spectrometry using a LTQ Orbitrap XL instrument (Thermo Scientific, Bremen, Germany) equipped with the automated nanoflow ion source Triversa NanoMate (Advion Biosciences, Ithaca, NY, USA) [28]. TO, POPC, TG 17:1/17:1/17:1 and PC 18:3/13:3 were detected by high-resolution Fourier transform mass spectrometry (FT MS) using a target mass resolution of 100,000. The abundance of TO and POPC was quantified using the internal standards TG 17:1/17:1/17:1 and PC 18:3/13:3, respectively, as previously described [29].

2.4. Small-angle X-ray scattering

Small-angle X-ray scattering (SAXS) experiments were performed on the prototype of the commercially available NanoStar camera (Bruker AXS) at Aarhus University [30]. The instrument uses a rotating anode source (Cu K-alpha) and a pair of Göbel multilayer mirrors. The beam is collimated by two pinholes where the one in front of the sample is defined by a set of homebuilt 'scatterless' hybrid slits following the principles described in [31]. The scattering is recorded by a position-sensitive gas proportional counter (HiSTAR, Bruker AXS). The instrument is optimised for solution scattering, has an integrated vacuum and employs a homebuilt semi-transparent beamstop for beam monitoring. The intensity is recorded as a function of the modulus of the scattering vector:

$$q = 4\pi sin(\theta)/\lambda \qquad (1)$$

where λ is the X-ray wavelength and θ is half the scattering angle. The samples were measured in reusable quartz capillaries sealed with steel caps and o-rings. The temperature was 25 °C and controlled by placing the capillary in a thermostated block. Water was measured as a background in the same capillary. The recorded intensities were

azimuthally averaged and the water signal was subtracted from the sample signal.

2.5. Electron paramagnetic resonance spectroscopy

EPR spectra were recorded on a Bruker EMX plus spectrometer (Bruker Biospin, Rheistetten, Germany). All spectra were recorded at 25 °C and the temperature was set by the internal temperature controller of the spectrometer. Before each experiment the temperature of the sample was checked with a small type K thermocouple attached to a Fluke 51 II thermometer (RS Components, Copenhagen, Denmark). All samples were measured in a micro hematocrit tube (Vitrex Medical A/S, Herlev, Denmark). The HF and LF were separated in the hematocrit tube by centrifugation in a Hettich 2010 hematocrit centrifuge (Andreas Hettich GmbH & Co. KG, Tuttlingen, Germany). The separated sample was placed in Wilmad Lab Glass standard 4 mm OD quartz EPR tube (Rotec Spintec GmbH, Griesheim, Germany) which was then mounted in the spectrometer. All spectra were recorded at X-band frequency (9.4 GHz) with a microwave power of 10 mW, a modulation frequency 100 kHz and with an amplitude of 1 G. The typical sweep time was 41 s. Usually 5 to 10 scans were summed in order to improve the signal-to-noise ratio.

2.5.1. Quantification of relative amounts of the HF and LF phases

The relative amounts of the HF and LF phases were estimated from double integral of the EPR spectra of the 16-PC spin-labels in the different POPC–TO samples. The amount of spin-labels is proportional to the double integral, so if the spin labels are equally distributed between the two phases, the double integral is also proportional to the amount of POPC in the two phases. We have chosen to use the 16-PC label as this showed a very small dependence on the presence of the TO and it has been shown that 16-PC does partition equally in to different lipid phases [32]. The EPR spectra were integrated using MATLAB R2010a (Mathworks, Natick, MA, USA) and the presented numbers are average of six independent samples.

2.5.2. Entrapped volume

The presence of an entrapped volume was investigated by a spin probe method. A lipid suspension, with a total lipid concentration of 80 mM, was prepared by hydrating a dried lipid film of the desired composition with a 0.1 mM solution of the water soluble, and not membrane binding, spin label tempamine [33]. The osmolarity of the tempamine solution was adjusted to approx. 150 mOsm with NaCl. The osmolarity was measured with a Gonotec Osmomat 30 (MD Scientific Aps, Aarhus, Denmark). The lipid suspensions were subjected to at least five freeze-thaw cycles using liquid N_2 to ensure equal distribution of the tempamine [34]. After this, the samples were separated by centrifugation into the HF and LF. The presence of an entrapped volume was then determined by an addition of a membrane impermeable quencher $K_3[Cr(Ox)_3]$ [35]. For the measurement 10 μL of the lipid suspension was mixed with 10 μL of af 50 mM K_3 $[Cr(Ox)_3]$ solution. The obtained spectrum was then compared with the spectrum obtained after the addition of 1 μL 20% Triton X-100, which converts any vesicular structures to micelles with no entrapped volume.

2.5.3. Order parameter measured with 5-PC and Me-5-DSA

Spin-labelled MLVs containing either 0.5 mol% Me-5-DSA or 0.3 mol% of the 5-PC spin label, were prepared and measured as described above. The order parameter was calculated from the hyperfine splittings (A_z and A_{xy}) by using the following equation [36]:

$$S = 0.5407 \frac{A_z - A_{xy}}{1/3(A_z + 2A_{XY})}. \qquad (2)$$

The presented numbers are average of six independent samples.

2.5.4. Membrane fluidity measured with 16-PC and Me-16-DSA

Spin-labelled MLVs containing either 0.5 mol% Me-16-DSA or 0.3 mol% of the 16-PC spin label, were prepared and measured as described above. Membrane fluidity was calculated using the following equation [37]:

$$\tau = kW\left((h/h)^{1-1}\right) \qquad (3)$$

where k is a constant, depending on the g and hyperfine splitting (A) of the nitroxide, h_0 is the line height of the central line, h_{-1} is the height of the high field line and W_0 the width of the central line. The presented numbers are average of six independent samples.

2.6. Nile red fluorescence emission spectra

Fluorescence emission spectra were recorded using an SLM Amico 8100 spectrophotometer (SLM Instruments, Urbana, IL, USA) at 25 °C. Temperature was maintained using a circulating waterbath (Julabo Labortechnik GmbH, Seelbach, Germany) and the temperature checked in the cuvette with a small type K thermocouple attached to a Fluke 51 II thermometer (RS Components, Copenhagen Denmark). The samples were excited at 540 nm. The excitation polariser was set to 90° and emission polariser to 0° to reduce the amount of scattered light. The probe concentration was 0.07 mol%. The HF samples were diluted 1:15 and the LF samples were measured undiluted. The spectra are averages of four scans, recorded with a scan rate of 1.5 nm min^{-1}. The presented numbers are average of four independent samples.

2.7. Laurdan generalised polarisation (GP) measurements

Fluorescence emission spectra were recorded as for the Nile red emission spectra except for the excitation wavelength, which was set to 370 nm. The GP values were calculated based on the equation [38]:

$$GP = \frac{I_{440} - I_{490}}{I_{440} + I_{490}} \qquad (4)$$

where I_{440} is the intensity at 440 nm and I_{490} is the intensity at 490 nm. The presented numbers are average of four independent samples.

2.8. Fluorescence microscopy

Fluorescence microscopy images of Nile red labelled samples were acquired using a Zeiss LSM 510 Meta NLO Confocal microscope (Carl Zeiss AG, Jena, Germany) at room temperature. The samples were illuminated using a 488 nm laser and the emitted light passing a 505 nm long pass filter was collected. The used objective was a 63× water immersion objective from Zeiss. All samples were prepared as for the fluorescence spectroscopy measurements.

2.9. Statistics

The presented numbers are the mean of three to six samples (see paragraphs above for details) and the reported error is the standard error (SE). Pair-wise statistical testing was performed using the non-parametric Kolmogorov–Smirnov test [39]. Confidence level was set to 0.05. Statistical analyses were made using the R software [40].
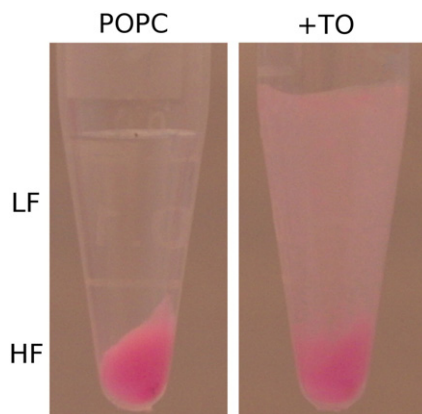
3. Results

We have earlier reported [25] that TO–POPC vesicles containing 10 mol% TO separate into two different phases upon centrifugation or overnight storage. Here we describe that the same behaviour also

applies to TO–POPC membranes prepared with 5 and 2 mol% TO. The phase forming a pellet at the bottom of the centrifugation tube we denote "HF" and the supernatant phase, a milky, mesh-like structure, LF following the nomenclature used earlier [25]. The LF phase was readily observed by spectroscopic means for all concentrations of TO, and for the samples prepared with 5 mol% and 10 mol% TO, this phase could also be easily seen by the eye, based on its milky appearance, see Fig. 1.
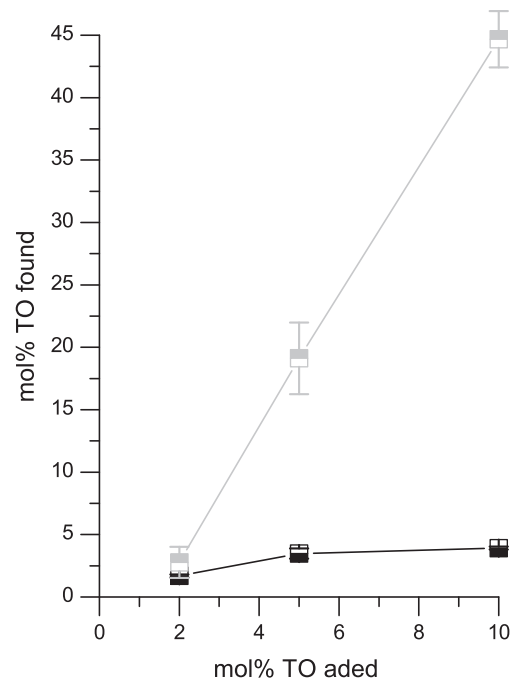
3.1. Composition

The composition of the POPC–TO samples after separation into the HF and LF phases was determined by quantitative mass spectrometry. The determined TO concentrations, as a function of the TO concentration used in sample preparation are shown in Fig. 2, where all compositions are given as mol% of the total amount of lipid in the sample. The two phases separated from the sample originally containing 2 mol% TO, did not differ in TO concentration after separation. Both contained around 2 mol% TO. For the samples where 5 or 10 mol% was originally used, a clear difference between the concentrations of TO in the HF and LF phases was observed. For the HF phases of the samples prepared with 5 mol% and 10 mol% TO, almost the same concentration of TO was found in both (3.5 ± 0.4 mol% and 3.9 ± 0.1 mol%, respectively). In the LF phases, the TO concentrations were found to be considerably higher, 19 ± 3 mol% and 45 ± 2 mol%, respectively, for 5% and 10 mol% original concentration.

In order to obtain an estimate for relative amounts of the two phases, we utilised EPR spectroscopy of the C-16 spin labelled phospholipid, 16-PC, (1-palmitoyl-2-stearoyl-(16-doxyl)-*sn*-glycero-3-phosphocholine). The relative amounts of HF and LF were estimated from the double integral of the EPR spectra, which is proportional to the amount of free spins in the sample. This again is proportional to the amount of POPC in each phase of the samples, if the partitioning coefficient of the spin label is the same in all phases. The 16-PC spin label has been found to have almost the same partitioning coefficient in both gel and fluid lipid membranes [32]. We therefore believe that the partition coefficient of 16-PC is of the same order for both the fluid HF and LF phases when considered in terms of phospholipids. The determined ratios of the double integrals as a function of the original TO concentration are shown in Fig. 3. It was observed that for the pure POPC, the amount of POPC in HF was 62 ± 20 times that of the LF, which was increased to around 82 ± 18 times for the samples where 2 mol% of TO was added. For the samples with 5 and 10 mol% original TO concentration ratio was in both cases around 24 (24 ± 4 and 24 ± 7, respectively). A statistically significant difference was found between the samples prepared with 2 mol% and
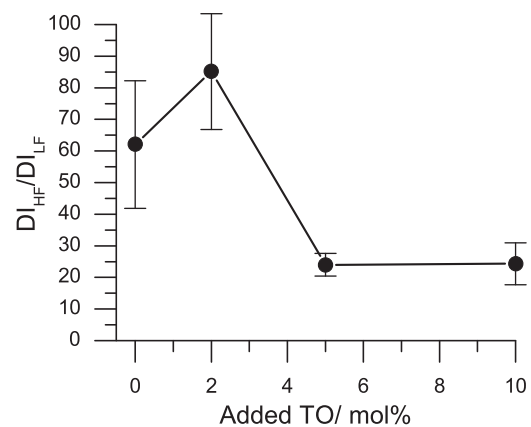

Fig. 2. TO concentration in the HF (black symbols) and LF (grey symbols) phases as a function of the amount of TO used in sample preparation before the two phases were separated. Numbers are mol% of the total lipid amount. The data shown are the mean of three independent samples and the error bar represents standard error (SE).

5 mol% ($P = 0.002$) and the sample with 10 mol% in the unseparated samples ($P = 0.02$).

3.2. Structure

As TO is present at high concentration in the LF phase, one cannot exclude the possibility for the phase to exist in an emulsion-like form: as TO droplets covered with a POPC monolayer. As such a structure, filled with TO would not contain any entrapped water – in contrast to vesicular bilayer structure – we utilised spin label quenching [34] to investigate if entrapped water was present in the two phases. For this experiment the samples were prepared in the presence of the watersoluble spin label TA (4-amino-2,2,6,6-tetramethylpiperidine-1-oxyl), that does not bind to or permeate a phospholipid membrane [33]. The TA outside of the lipid structure was then quenched by the

Fig. 1. Centrifuged, Nile red labelled samples of pure POPC and POPC containing 10 mol% of TO. In both samples a pellet is clearly seen. It is referred to as the HF phase. In the sample with 10 mol% TO the milky supernatant phase, LF, is clearly visible.


Fig. 3. The ratio of the double integral (DI) of the EPR spectra of the 16-PC spin-label in the HF and LF phases as a function of the TO concentration in the unseparated samples. This ratio corresponds to the ratio of POPC amounts in the two phases. Numbers are means of six independent samples and the error bar represents SE.

addition of a quencher which cannot cross the membrane, giving an EPR spectrum of only the entrapped TA, if present. $K_3[Cr(Ox)_3]$ was used as quencher [35] and finally Triton-X-100, a non-ionic surfactant, was added, resulting in destruction of any vesicular structures. In the presence of any structure with entrapped volume, the signal intensity of the $K_3[Cr(Ox)_3]$ quenched spectra would be higher than the spectra recorded in the presence of both of Triton-X-100 and $K_3[Cr(Ox)_3]$. Therefore a marked difference between the intensities of these two spectra was taken as an indication of the presence of an entrapped volume. For the HF phases of all TO concentrations an entrapped water volume was found, indicating the presence of vesicular structures. For the LF we were only able to observe an entrapped volume for the samples prepared with 5 or 10 mol% TO, i.e., samples containing 19 or 45 mol% TO. For the LF prepared with 0 or 2 mol% TO we were not able to observe an entrapped volume. The spectra obtained are shown in Supplementary Material Fig. 1.

To support the EPR results and to obtain a more detailed view on the structure of the TO–POPC membranes, we utilised small-angle X-ray scattering (SAXS). The scattering curves, shown in Fig. 4, showed for all the investigated samples the presence of multilamellar structures as seen by the presence of Bragg peaks at q_{lam} and $2q_{lam}$ in the scattering patterns. The signal intensity was markedly lower for all the LF than for the HF phase, which is in good accordance with all the other experiments. For the LF samples prepared with an original concentration of 0 and 2 mol% TO very weak, almost not observable, peaks were seen. For the LF prepared with 5 and 10 mol% TO added, two peaks were clearly seen, with the peak located roughly at the same positions. The low signal to noise ratio did not allow a precise determination of the peak position. For all the HFs two clear peaks were observed. The peaks moved to slightly lower q-values with increasing amount of TO, which indicated a slightly increased lamellar spacing.
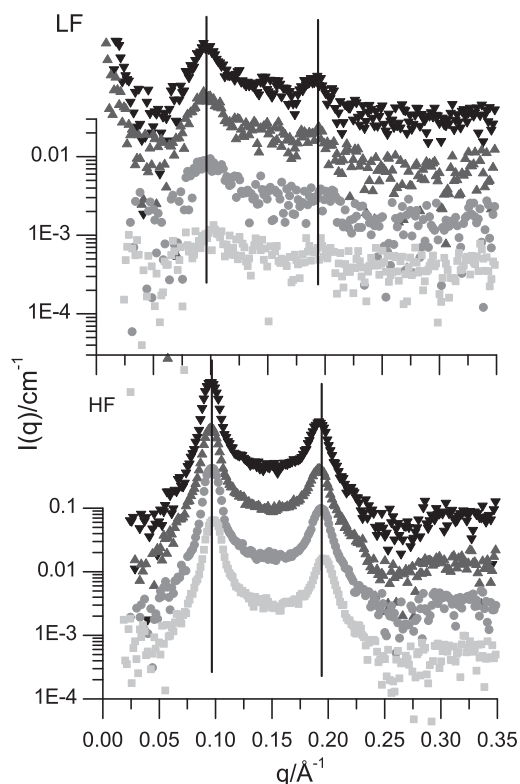
Fig. 4. Scattering intensity (I) as a function of the scattering vector (q) for the LF (top) and HF (bottom) phases. Black points: 10 mol% TO, dark grey points: 5 mol% TO, grey points: 2 mol% TO used in sample preparation before separation. Light grey points: pure POPC. Measurements are offset by a factor of 5 between each sample.

In order to investigate the large scale morphology of the POPC–TO samples, a series of confocal images of samples labelled with Nile red were obtained. Representative images are shown in Fig. 5. All the HF samples contained a rather high amount of lipid structures with varying geometry, as typically seen for multilamellar vesicles (MLVs). The samples with the higher amounts of TO had a tendency to form more tubular structures. LF samples featured generally smaller sized structures and were less particulate than those of the HF but as the concentration of TO was increased more particles were seen in the samples, and the geometry seemed to be more varying and the structures are slightly larger.

3.3. Spectroscopy

We have earlier proposed a model for the organisation of TO in the POPC membrane based on molecular dynamics simulations. Intriguingly, in these simulations, at TO concentrations above 2–5 mol%, TO seemed to aggregate inside the POPC bilayer forming a "blister" domain [26]. In the present study we investigated the bilayer properties of the TO–POPC membranes in the effort to provide experimental evidence for the existence of the blister domains by using spectroscopical methods.

3.3.1. EPR

EPR, a method sensitive to the intramolecular motions of an added spin label, can reveal details about the local properties of a membrane [36,41]. The local order parameter, S, can be determined from the EPR spectra of the 1-palmitoyl-2-stearoyl-(5-doxyl)-sn-glycero-3-phosphocholine (5-PC) and methyl-5-doxylstearic acid (Me-5-DSA) spin-labels. This describes the organisation of the membrane by the time-averaged fluctuation of the acyl chain segment relative to the bilayer normal, hence providing information on the degree of acyl chain order [36,41].

Here the order parameters of the studied membranes were calculated from the spectra of the Me-5-DSA and 5-PC spin labels at 25 °C. These results are shown as a function of the found TO concentration in Fig. 6. The order parameters calculated from the spectra of the 5-PC label showed no variation with the found TO concentration, but for all TO concentrations, as well as for pure POPC, a small difference in S between the HF and LF was found. This did not apply to S calculated from the Me-5-DSA spectra where the HFs had a tendency for a lower S in the case of 5 and 10 mol% TO in unseparated samples compared to pure POPC. For the LF we were not able to observe an analysable EPR spectrum for the pure POPC sample, probably due to the generally lower intensity of the Me-5-DSA labelled samples. For the LF samples containing 2 and 19 mol% TO we found $S \approx 0.36$ for both concentrations whereas for the sample containing 44.6 mol% we found statistically significant lower values of $S = 0.257 \pm 0.004$ ($P = 0.002$).

From the EPR spectra of the 16-PC and methyl-16-doxylstearic acid (Me-16-DSA) spin-labels in the membranes it is possible to determine the rotational correlation time, τ. This can be viewed as a measure of the fluidity of the membrane [42], since τ is inversely proportional to the microviscosity of the membrane, according to the Stokes–Einstein equation. In the present work fluidity has been defined as the inverse of the local viscosity of the membrane. The rotational correlation time calculated from the spectra measured with Me-16-DSA and 16-PC spin labels are shown in Fig. 6 as a function of the determined TO concentration. For the HF phase the 16-PC spectra gives an almost constant value of $\tau = 2.4$ ns for all TO concentrations, whereas we in the case of the Me-16-DSA labelled samples observed a small, but statistically significant, increase in τ from 2.20 ± 0.04 ns for the pure POPC to 2.30 ± 0.01 ns for a TO concentration of 3.9 mol%. Due to the large variation in the data no statistical difference was found for the LF phase. Nevertheless, the general trend for the samples with 16-PC label was fairly unchanged with
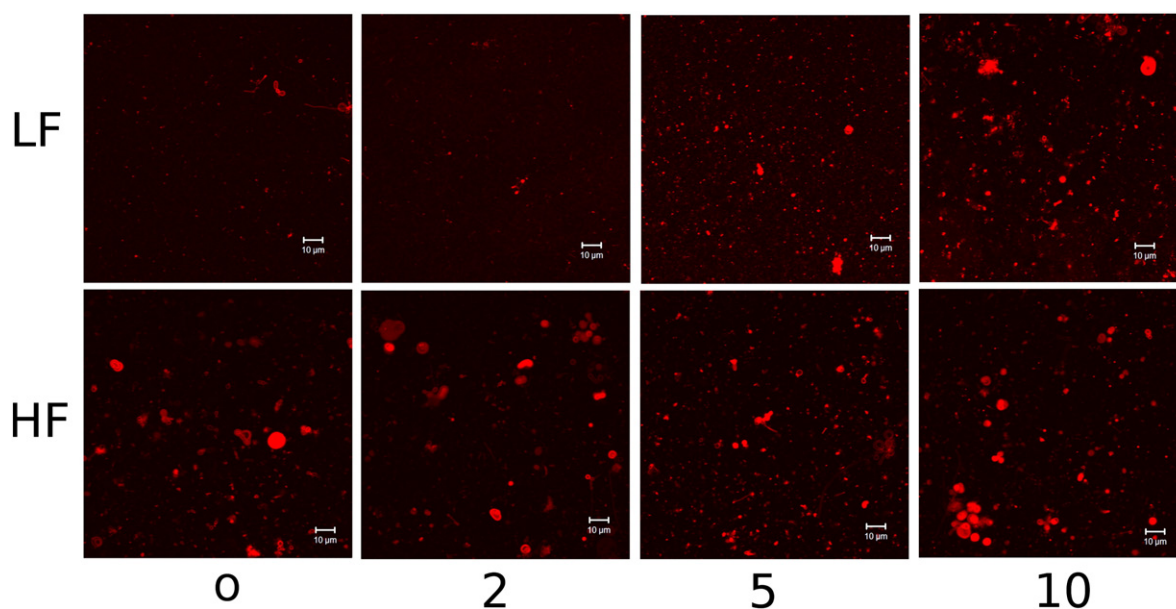
Fig. 5. Nile red labelled TO–POPC samples of the LF (top) and HF (bottom) phases. Numbers refer to mol% in the unseparated samples.

$\tau \approx 2.35$ ns opposite to a slight decrease from $\tau = 2.33$ ns to around $\tau = 2.16$ ns seen for the Me-16-DSA labelled samples.

3.3.2. Fluorescence spectroscopy

As the proposed blister domains structurally resemble lipid droplets (with the exception of not being released from the membrane)

[26], we used a classical lipid droplet dye, Nile red (9-diethylamino-5-benzo[α]phenoxazinone), to gain information on the existence of the proposed droplet domains. Nile red is commonly used for the identification of lipid droplets in cells [43], due to its polarity sensitive emission properties [44,45]. In a triglyceride-rich environment, like inside a lipid droplet, the emission maximum of Nile red is at 571 nm
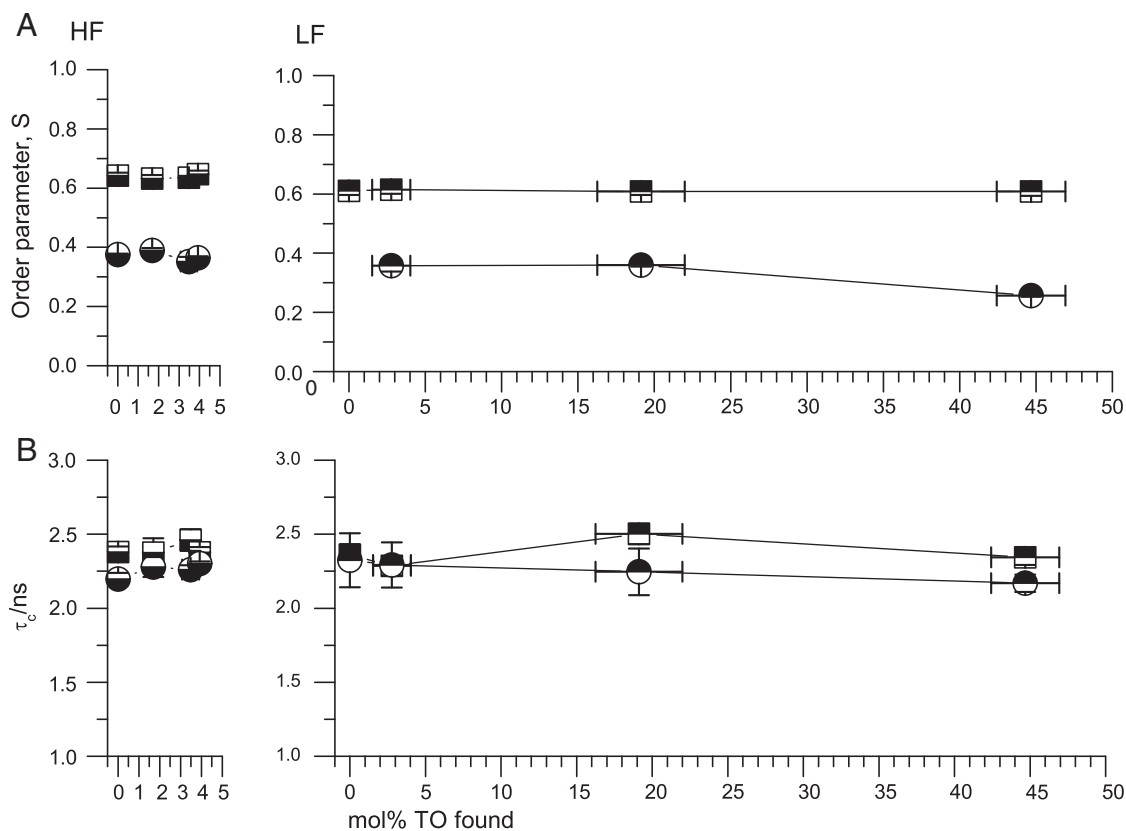

Fig. 6. Molecular order parameter, S as a function of the amount of TO in the different phases (A). S was calculated from the spectra of carbon-5 labelled spin labels. Correlation time (τ_c) as a function of the found TO concentration in the different phases (B) was calculated from the carbon-16 labelled spin label. Circles: Me-5/16-DSA probe, square:5/16-PC probe. Grey, upper part filled: LF. Black, lower part filled: HF. Numbers are the mean of six independent samples and the error bar represents SE.

while it in a phospholipid membrane has an emission maximum at 623 nm. This shift of emission maximum forms the basis for the identification of lipid droplets, both in microscopy and spectroscopy.

Nile red emission spectra of the different TO–POPC mixtures are shown in Fig. 7 (A for HF and B for LF). All the HF spectra were identical and had an emission maximum at 623 nm, indicating that Nile red was located in a phospholipid membrane environment. For the LFs, the samples prepared with 0 and 2 mol% TO presented spectra similar to HF whereas the samples prepared with 5 and 10 mol% TO showed a clearly increased intensity around 571 nm and for the sample prepared with 10 mol% TO the intensity at 571 nm was almost the same as at 623 nm.

In order to quantify this shift, the ratio between the intensity at 571 nm and 623 nm was calculated, and is shown in Fig. 7C. For the HFs, a ratio of around 0.32 was found for all the investigated samples. Small but statistically significant differences were found between the pure POPC (ratio = 0.314 ± 0.002) and the HF in the samples prepared with 5 mol% TO (ratio = 0.323 ± 0.002, P = 0.029) and between the pure POPC and the sample prepared with 10 mol% TO (ratio = 0.335 ± 0.005, P = 0.029). For the LF phase a linearly increasing 571/623 nm ratio was found, ranging from 0.323 ± 0.007 in the pure sample to 0.94 ± 0.09 for the samples containing 45 mol% TO (originally 10 mol% in unseparated sample). The differences between all LF samples were found to be statistically significant (P = 0.03) and, with the exception of the pure POPC samples, significantly different from all the HF samples (P = 0.03).

Highly hydrophobic blister domains located inside a membrane could attract molecules with highly hydrophobic tail and weakly hydrophilic head to partition inside the blister. We have earlier proposed the fluorescent probe Laurdan (6-dodecanoyl-2-dimethylaminonaphthalene) to be such a molecule [26]. With the new results for Nile red, we used Laurdan to investigate the polarity of its local environment in TO–POPC membranes. The emission properties of the fluorescence dye Laurdan, is affected by the dipolar relaxations in the surrounding solvent. In lipid membranes the fluorescence naphthalene moiety of Laurdan is located at the level of the glycerol backbone, where also water molecules can penetrate in a fluid membrane. Upon excitation the surrounding dipoles the water molecules will align with the naphthalene unit and thereby some of the excited state energy is transferred to the surroundings which leads to a red-shift in the emission spectra [38]. Generalised polarisation, GP, can be calculated from the emission spectra. The number can be considered as inversely proportional to the amount of water surrounding the Laurdan molecules.

GP values calculated from Laurdan emission spectra are shown in Fig. 7D. For the HF of pure POPC we found a GP of 0.012 ± 0.000, which increased slightly, up to 0.034 ± 0.002 for the sample containing 3.9 mol% TO. A larger variation in GP was seen with the LFs. For the pure POPC sample we found GP = −0.05 ± 0.03. This increased to 0.03 ± 0.03 for the sample containing 2.7 mol% and to 0.07 ± 0.04 for the sample with 19.1 mol% TO. The LF sample containing 45 mol% TO (10 mol% in unseparated sample) gave a
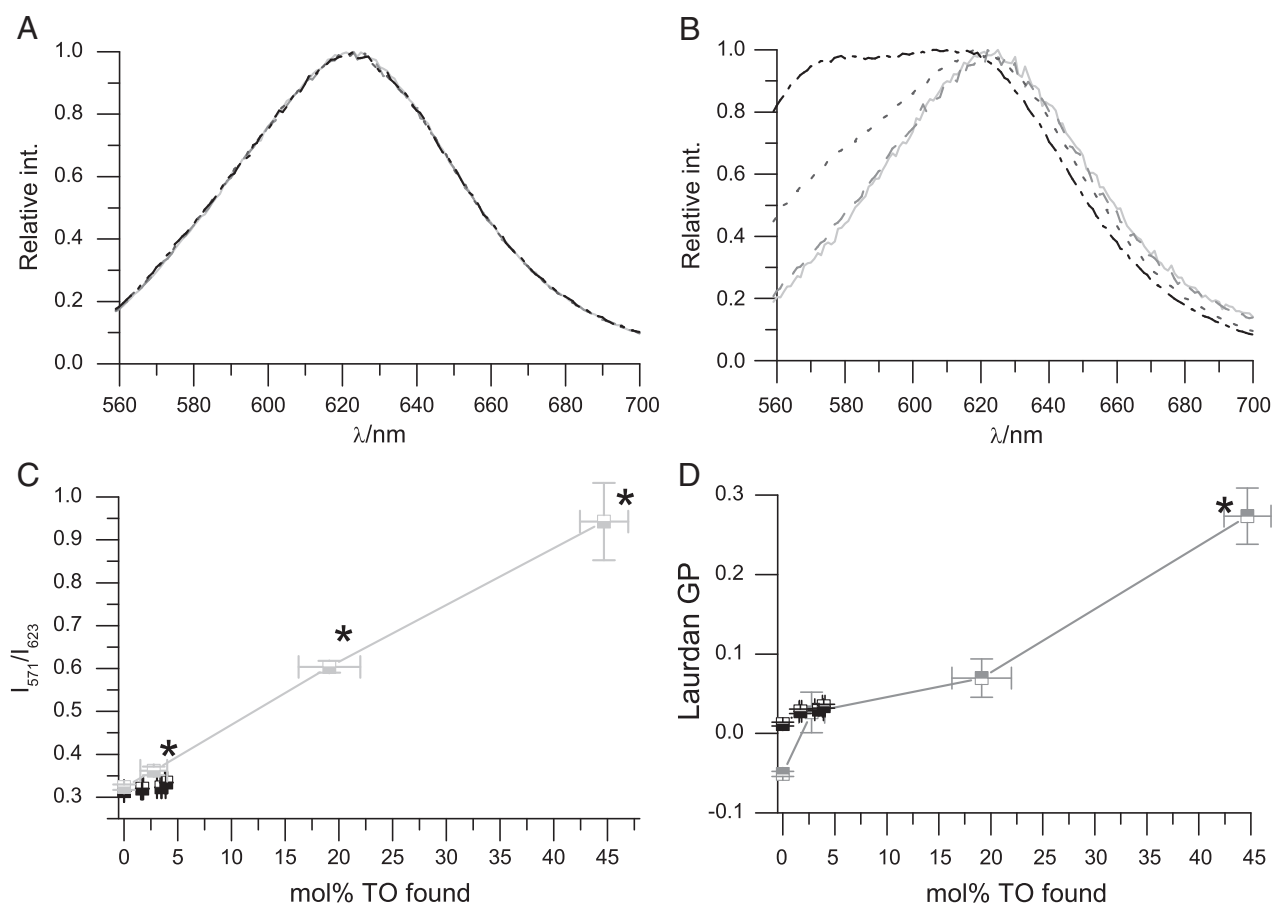
Fig. 7. Normalised emission spectra of the Nile red labelled membranes in the HF (A) and LF (B) phases. The spectra were normalised to maximum intensity of 1. Black line: 10 mol% TO, dark grey line: 5 mol% TO, grey line: 2 mol% TO (original concentration in unseparated samples) and light grey line: pure POPC. C) Ratio of the intensity at 571 nm over the intensity at 623 nm. D) General polarisation, GP, as a function of the found TO concentration in the different phases. Grey, top filled: LF. Black, lower part filled: HF. All numbers are the mean of four samples. The error bar represents SE.

GP $= 0.27 \pm 0.4$, which was significantly different from all other GP-values ($P = 0.04$ in all cases).

4. Discussion

In line with our previous work [25] we found that POPC–TO mixtures separate into two distinct phases upon centrifugation. In this work we found that the amount of the light phase (LF) was higher for the samples prepared with 5 or 10 mol% TO. This could be seen by both eye (Fig. 1) and spectroscopic means (Fig. 3).

In order to fully understand the origin of these two phases precise knowledge of the composition is needed. We therefore investigated the composition of the two phases by quantitative mass spectrometry. The TO concentration found in the HF phase indicated that the solubility limit of TO was approximately 4 mol%, which is in agreement with both our previous work [25] and previously published NMR work [19,20] where a maximum solubility of 2.8 mol% of TO in egg phospatidylcholine membranes was found. In contrast to this we found a marked up-concentration of TO in the LF phase, relative to the original concentrations of TO used in the sample preparation (19 mol% and 45 mol% for the samples prepared with 5 and 10 mol% TO, respectively). This is markedly different from our previous findings [25], where we found no up-concentration of the TO in the LF phase. As the new compositional data is obtained by mass spectrometry, a technique with significant better dynamic range and a lower detection limit, we believe this new data to represent the situation more accurately. This new data also provides a better explanation of the separation into the two phases than the earlier numbers.

With the high concentration of TO found in the LF phase it is not obvious that this phase is organised as vesicular lipid bilayers. For a mixture of this composition an emulsion-like structures could easily be envisioned. A fundamental difference between an emulsion and a vesicular structure is the presence of an entrapped water volume inside the vesicles. We used EPR signal quenching to test if the TO-rich LF phases contained entrapped water as indication of vesicular structure [34]. With HF fractions we found an entrapped volume for all compositions. We were also able to observe an entrapped volume for LF samples prepared with 5 or 10 mol% TO. This indicates that also these LF phases containing 19 and 45 mol% TO are in a vesicular state. It was not possible to detect an entrapped volume in the LF samples prepared with 2 mol% TO or with POPC only. We strongly believe that this is due to the very low amount of lipids in the samples, leading to a small amount of entrapped volume and thus a low signal. For the HF phases of the same composition (0 and 2 mol% TO) an entrapped volume was detected.

The detailed arrangement of the TO–POPC structures were also studied by SAXS measurements. This showed that the HF phases of all the investigated samples have a multilamellar structure. We observed weak peaks characteristic for multilamellar structures in LF samples indicating multilamellar organisation. The low signal to noise ratio of the LF phase did not allow a reliable determination of the peak position from the SAXS data, but we can estimate that the lamellar repeat distance for all the LFs are close to identical. For the HF phase a slight increase in the lamellar repeat distance with increasing amounts of TO in the membranes was observed. This is consistent with the increased lamellar spacings found for the samples prepared with 10 mol% of TO published earlier [27].

Further indication of organisation of the TO–POPC lipid mixtures as vesicular structures came from fluorescence microscopy. In the fluorescence microscopy images (Fig. 5) we observed in all cases a varying amount of up to micrometre sized objects, which were markedly larger than what could be expected with either micellar or emulsion-like structures. The varying amounts of structures observed by visual inspection are in agreement with the results of the EPR spectroscopy (Fig. 3). The vesicular arrangement of the lipids is also consistent with previously published TEM images [27].

As our results indicate the lipids of the TO–POPC mixtures to be arranged in lamellar lipid bilayers, we need to consider how the high amount of TO molecules could be arranged in the membrane. In the previously published molecular dynamics (MD) simulations by us and our-coworkers [26] the TO molecules at low concentrations (2.3 mol%) were found at the water–membrane interface whereas at a higher concentration (5.2 mol%) TOs were present not only at the water–membrane interface but also as blister-like domains inside the bilayer [26]. Based on our present results and the earlier MD simulation study, it is tempting to speculate that TO in the HF phase could be located on the water–membrane interface similar to the case of low TO concentration in the MD simulations, whereas TO in the LF phase would be arranged mainly in blister domains. Our EPR results strengthened by fluorescence spectroscopy studies with Nile red support this view. Nile red is commonly used to detect lipid droplets in cells [43] as its emission spectrum depends on the polarity of the surrounding environment. The obtained emission spectra for all the samples with less than 4 mol% of TO were identical to the spectra obtained with pure POPC, see Fig. 7. The samples containing higher concentrations of TO showed a peak developing at 571 nm, which is indicative of the Nile red probe being located in an almost pure triglyceride phase. This is consistent with the observations with both the Laurdan GP measurements and EPR spectroscopy. The calculated GP values were as expected for a fluid bilayer [38] and showing a small, non-significant increase up to 20 mol% TO indicates that Laurdan is placed in a nearly unperturbed lipid bilayer. The significantly higher GP value found samples containing 45 mol% of TO (10 mol% original concentration) can be interpreted as a result of some the Laurdan molecules leaving the lipid bilayer and partitioning into TO domains. Also the EPR spectroscopy is consistent with this. When we probed the TO–POPC bilayers with spin-labelled PC lipids that are, due to their phospholipid structure, strongly anchored to the membrane, we could not detect any difference in the measured properties of the bilayer. In contrast, when the bilayer was probed with Me-5-DSA, as small decrease in the order parameter, relative to the pure POPC membrane, was seen. This could indicate that the poorly-anchored probe leaving its normal membrane location and partitioning into the highly apolar TO domains inside the bilayer, as seen for Laurdan.

We have here by a range of experimental techniques, obtained a set of results that all support the interpretation that TO, at a concentration above 4 mol%, is arranged in blister-like domains between the two leaflets of the membrane bilayers as we, together with our co-workers, have suggested earlier [26]. This arrangement of TO in between the lipid monolayers of the bilayer membrane has been speculated as the first step in the formation of lipid droplets [3,46] and to be the origin of the so-called mobile lipid domains in cancer cells [12]. Until now, however, very little evidence for this arrangement has been presented. With the presented study we have given evidence for such an intra-bilayer domain arrangement to be possible. The model system used in these studies can be used for further investigations e.g. to elucidate the role of the different components in lipid droplet formation, and for the properties of the mobile lipid domains in cancerous cells.

Appendix A. Supplementary data

Supplementary data to this article can be found online at http://dx.doi.org/10.1016/j.bbamem.2013.03.020.

References

[1] R.V. Farese Jr., T.C. Walther, Lipid droplets finally get a little respect, Cell 139 (5) (2009) 855–860.

[2] Y. Guo, K.R. Cordes, R.V. Farese Jr., T.C. Walther, Lipid droplets at a glance, J. Cell Sci. 122 (6) (2009) 749–752.

[3] M. Suzuki, Y. Shinohara, Y. Ohsaki, T. Fujimoto, Lipid droplets: size matters, J. Electron Microsc. 60 (Suppl. 1) (2011) S101–S116.

[4] J. Stanley, Lipoproteins. 1. Physiological roles and structure, Lipid Technol. 13 (2001) 41–44.

[5] J. Heeren, U. Beisiegel, Intracellular metabolism of triglyceride-rich lipoproteins, Curr. Opin. Lipidol. 12 (3) (2001) 255.

[6] J.A. Higgins, J.L. Hutson, The roles of golgi and endoplasmic reticulum in the synthesis and assembly of lipoprotein lipids in rat hepatocytes, J. Lipid Res. 25 (12) (1984) 1295–1305.

[7] M. Hills, T. Roscoe, Synthesis of structural and storage lipids by the ER, The Plant Endoplasmic Reticulum, Springer, 2006, pp. 155–186.

[8] J. Brotherus, O. Renkonen, Subcellular distributions of lipids in cultured bhk cells: evidence for the enrichment of lysobisphosphatidic acid and neutral lipids in lysosomes, J. Lipid Res. 18 (2) (1977) 191–202.

[9] T. Kobayashi, E. Stang, K.S. Fang, P. de Moerloose, R.G. Parton, J. Gruenberg, A lipid associated with the antiphospholipid syndrome regulates endosome structure and function, Nature 392 (6672) (1998) 193–197.

[10] J. Gil, O.K. Reiss, Isolation and characterization of lamellar bodies and tubular myelin from rat lung homogenates, J. Cell Biol. 58 (1) (1973) 152–171.

[11] G.L. May, L.C. Wright, K.T. Holmes, P.G. Williams, I.C. Smith, P.E. Wright, R.M. Fox, C.E. Mountford, Assignment of methylene proton resonances in NMR spectra of embryonic and transformed cells to plasma membrane triglyceride, J. Biol. Chem. 261 (7) (1986) 3048–3053.

[12] C.E. Mountford, L.C. Wright, Organization of lipids in the plasma membranes of malignant and stimulated cells: a new model, Trends Biochem. Sci. 13 (1988) 172–177.

[13] A. Ferretti, A. Knijn, E. Iorio, S. Pulciani, M. Giambenedetti, A. Molinari, S. Meschini, A. Stringaro, A. Calcabrini, I. Freitas, et al., Biophysical and structural characterization of ^{1}H-NMR-detectable mobile lipid domains in NIH-3T3 fibroblasts, Biochim. Biophys. Acta 1438 (3) (1999) 329–348.

[14] C. Rémy, N. Fouilhé, I. Barba, E. Sam-Laï, H. Lahrech, M. Cucurella, A. Izquierdo, A. Moreno, A. Ziegler, R. Massarelli, et al., Evidence that mobile lipids detected in rat brain glioma by ^{1}H nuclear magnetic resonance correspond to lipid droplets, Cancer Res. 57 (3) (1997) 407.

[15] J.M. Hakumäki, R.A. Kauppinen, ^{1}H NMR visible lipids in the life and death of cells, Trends Biochem. Sci. 25 (8) (2000) 357–362.

[16] E.J. Delikatny, S. Chawla, D.J. Leung, H. Poptani, MR-visible lipids and the tumor microenvironment, NMR Biomed. 24 (2011) 592–611.

[17] O.G. Mouritsen, M.J. Zuckermann, What's so special about cholesterol? Lipids 39 (11) (2004) 1101–1113.

[18] L.A. Bagatolli, J.H. Ipsen, A.C. Simonsen, O.G. Mouritsen, An outlook on organization of lipids in membranes: searching for a realistic connection with the organization of biological membranes, Prog. Lipid Res. 49 (4) (2010) 378–389.

[19] J.A. Hamilton, D.A. Small, Solubilization and localization of triolein in phosphatidylcholine bilayers: a ^{13}C NMR study, Proc. Natl. Acad. Sci. U. S. A. (11) (1981) 6878–6882.

[20] J.A. Hamilton, K.W. Miller, D.M. Small, Solubilization of triolein and cholesteryl oleate in egg phosphatidylcholine vesicles, J. Biol. Chem. 258 (21) (1983) 12821–12826.

[21] J.A. Hamilton, D.T. Fujito, C.F. Hammer, Solubilization and localization of weakly polar lipids in unsonicated egg phosphatidylcholine: a carbon-13 MAS NMR study, Biochemistry 30 (11) (1991) 2894–2902.

[22] P.J.R. Spooner, D.M. Small, Effect of free cholesterol on incorporation of triolein in phospholipid bilayers, Biochemistry 26 (18) (1987) 5820–5825.

[23] R. Li, W. Schmidt, S. Rankin, R.L. Walzem, E. Boyle-Roden, Solubilization of acyl heterogeneous triacylglycerol in phosphatidylcholine vesicles, J. Agric. Food Chem. 51 (2) (2003) 477–482.

[24] J.M. Smaby, H.L. Brockman, Regulation of cholesteryl oleate and triolein miscibility in monolayers and bilayers, J. Biol. Chem. 262 (17) (1987) 8206–8212.

[25] K.I. Pakkanen, L. Duelund, M. Vuento, J.H. Ipsen, Phase coexistence in a triolein-phosphatidylcholine system. Implications for lysosomal membrane properties, Chem. Phys. Lipids 163 (2) (2010) 218–227.

[26] H. Khandelia, L. Duelund, K.I. Pakkanen, J.H. Ipsen, Triglyceride blisters in lipid bilayers: implications for lipid droplet biogenesis and the mobile lipid signal in cancer cell membranes, PLoS One 5 (9) (2010) e12811.

[27] K.I. Pakkanen, L. Duelund, K. Qvortrup, J.S. Pedersen, J.H. Ipsen, Mechanics and dynamics of triglyceride-phospholipid model membranes: implications for cellular properties and function, Biochim. Biophys. Acta 1808 (8) (2011) 1947–1956.

[28] C.S. Ejsing, J.L. Sampaio, V. Surendranath, E. Duchoslav, K. Ekroos, R.W. Klemm, K. Simons, A. Shevchenko, Global analysis of the yeast lipidome by quantitative shotgun mass spectrometry, Proc. Natl. Acad. Sci. U. S. A. 106 (7) (2009) 2136–2142.

[29] C.S. Ejsing, E. Duchoslav, J.L. Sampaio, K. Simons, R. Bonner, C. Thiele, K. Ekroos, A. Shevchenko, Automated identification and quantification of glycerophospholipid molecular species by multiple precursor ion scanning, Anal. Chem. 78 (17) (2006) 6202–6214.

[30] J.S. Pedersen, A flux-and background-optimized version of the nanostar small-angle X-ray scattering camera for solution scattering, J. Appl. Crystallogr. 37 (3) (2004) 369–380.

[31] Y. Li, R. Beck, T. Huang, M.C. Choi, M. Divinagracia, Scatterless hybrid metal-single-crystal slit for small-angle X-ray scattering and high-resolution X-ray diffraction, J. Appl. Crystallogr. 41 (6) (2008) 1134–1139.

[32] Y.-C. Lai, Y.-W. Chiang, Asymmetric partition of spin labeled lipids in the coexistence of DPPC-rich ordered and DLPC-rich fluid phases, Chin. J. Magn. Reson. 27 (3) (2010) 470–484.

[33] J. Fuchs, W.H. Nitschmann, L. Packer, O.H. Hankovszky, K. Hideg, pK_a values and partition coefficients of nitroxide spin probes for membrane bioenergetics measurements, Free Radical Res. 10 (6) (1990) 315–323.

[34] W.R. Perkins, S.R. Minchey, P.L. Ahl, A.S. Janoff, The determination of liposome captured volume, Chem. Phys. Lipids 64 (1–3) (1993) 197–217.

[35] S.P. Berg, D.M. Nesbitt, Chromium oxalate: a new spin label broadening agent for use with thylakoids, Biochim. Biophys. Acta 548 (3) (1979) 608–615.

[36] W.K. Subczynski, M. Raguz, J. Widomska, Studying lipid organization in biological membranes using liposomes and EPR spin labeling, Methods in Molecular Biology, vol. 606, 2010, pp. 247–269, (Ch. 18).

[37] P.L. Nordio, General magnetic resonance theory, in: L.J. Berliner (Ed.), Spin Labeling, Theory and Applications, Academic Press, New York, 1976, pp. 5–52, (Ch. 2).

[38] T. Parasassi, G. De Stasio, A. d'Ubaldo, E. Gratton, Phase fluctuation in phospholipid membranes revealed by Laurdan fluorescence, Biophys. J. 57 (6) (1990) 1179–1186.

[39] NIST, http://www.itl.nist.gov/div898/handbook/NIST/SEMATECH e-Handbook of Statistical Methods. URL http://www.itl.nist.gov/div898/handbook/2011.

[40] R Development Core Team, http://www.R-project.org/R: A Language and Environment for Statistical Computing, R Foundation for Statistical Computing, Vienna, Austria3-900051-07-0, 2011. (URL http://www.R-project.org/).

[41] D. Marsh, Electron spin resonance, in: E. Grell (Ed.), Membrane Spectroscopy, Springer-Verlag, Berlin, 1981, pp. 51–142.

[42] D. Marsh, ESR probes for structure and dynamics of membranes, in: P.M. Bayley, R.E. Dale (Eds.), Spectroscopy and the Dynamics of Molecular Biological Systems, Academic Press, London, 1985, pp. 209–238.

[43] P. Greenspan, E.P. Mayer, S.D. Fowler, Nile red: a selective fluorescent stain for intracellular lipid droplets, J. Cell Biol. 100 (3) (1985) 965.

[44] P. Greenspan, S.D. Fowler, Spectrofluorometric studies of the lipid probe, Nile red, J. Lipid Res. 26 (7) (1985) 781–789.

[45] P.J.G. Coutinho, Photophysics and biophysical applications of benzo[a]phenoxazine type fluorophores, Rev. Fluoresc. (2009) 335–362.

[46] T.C. Walther, R.V. Farese, The life of lipid droplets, Biochim. Biophys. Acta 1791 (6) (2009) 459–466.